




OPEN

# The coral reef-dwelling *Peneroplis* spp. shows calcification recovery to ocean acidification conditions

Laurie M. Charrieau<sup>1,2</sup>, Yukiko Nagai<sup>1,3</sup>, Katsunori Kimoto<sup>4</sup>, Delphine Dissard<sup>5</sup>, Beatrice Below<sup>5,6</sup>, Kazuhiko Fujita<sup>7</sup> & Takashi Toyofuku<sup>1,8</sup>

Large Benthic Foraminifera are a crucial component of coral-reef ecosystems, which are currently threatened by ocean acidification. We conducted culture experiments to evaluate the impact of low pH on survival and test dissolution of the symbiont-bearing species *Peneroplis* spp., and to observe potential calcification recovery when specimens are placed back under reference pH value (7.9). We found that *Peneroplis* spp. displayed living activity up to 3 days at pH 6.9 ( $\Omega_{\text{cal}} < 1$ ) or up to 1 month at pH 7.4 ( $\Omega_{\text{cal}} > 1$ ), despite the dark and unfed conditions. Dissolution features were observed under low  $\Omega_{\text{cal}}$  values, such as changes in test density, peeled extrados layers, and decalcified tests with exposed organic linings. A new calcification phase started when specimens were placed back at reference pH. This calcification's resumption was an addition of new chambers without reparation of the dissolved parts, which is consistent with the porcelaneous calcification pathway of *Peneroplis* spp. The most decalcified specimens displayed a strong survival response by adding up to 8 new chambers, and the contribution of food supply in this process was highlighted. These results suggest that porcelaneous LBF species have some recovery abilities to short exposure (e.g., 3 days to 1 month) to acidified conditions. However, the geochemical signature of trace elements in the new calcite was impacted, and the majority of the new chambers were distorted and resulted in abnormal tests, which might hinder the specimens' reproduction and thus their survival on the long term.

Anthropogenic carbon dioxide (CO<sub>2</sub>) emissions in the atmosphere are consistently increasing, which is driving the current climate change including the ocean acidification (OA) phenomenon<sup>1–3</sup>. The majority of calcifying marine organisms are negatively affected by OA and display decreased survival, calcification rate, growth and abundance when living under OA conditions<sup>4,5</sup>. However, some species appear not to be affected or even benefit from OA conditions, and thus the response of calcifiers to OA is complex and depends on several parameters such as their life stage, nutritional status, protective organic covering, pH regulation and photosynthesis abilities<sup>4–6</sup>. Moreover, local adaptation and adaptive plasticity appear to have a role in the species resilience to OA<sup>7</sup>. Coral reefs were among the first ecosystems to be recognized as threatened by OA<sup>8</sup>, and models predict heterogeneous but rapid degradation of coral reefs worldwide under future climate change scenarios<sup>9–11</sup>.

Large Benthic Foraminifera (LBF) are calcifying protists dwelling in warm coral reef environments, where they contribute to almost 5% of the annual present day calcium carbonate production<sup>12,13</sup>. Most modern LBF are hosts of algal symbionts, which provide them a valuable source of energy through photosynthesis<sup>14,15</sup>. This photosynthetic activity locally increases pH around the foraminifera, which partially protect them but does not fully compensate for OA conditions<sup>16,17</sup>. Foraminifera are also known to have a tight control of their internal and external pH during the calcification process<sup>18–20</sup>. Benthic foraminifera are widely used in fossil and modern records as biostratigraphic markers and bioindicators, including in coral-reef environments<sup>21–23</sup>. Furthermore,

<sup>1</sup>Institute for Extra-Cutting-Edge Science and Technology Avant-Garde Research (X-STAR), Japan Agency for Marine-Earth Science and Technology (JAMSTEC), Natsushima-cho 2-15, Yokosuka 237-0061, Japan. <sup>2</sup>Marine Biogeosciences, Alfred Wegener Institute (AWI), Am Handelshafen 12, 27570 Bremerhaven, Germany. <sup>3</sup>National Museum of Nature and Science, 4-1-1 Amakubo, Tsukuba 305-0005, Japan. <sup>4</sup>Research Institute for Global Change (RIGC), Japan Agency for Marine-Earth Science and Technology (JAMSTEC), Natsushima-cho 2-15, Yokosuka 237-0061, Japan. <sup>5</sup>IRD/UMR LOCEAN (IRD-CNRS-MNHN-Sorbonne Université), Centre IRD de Nouméa, 101 Promenade Roger Laroque, 98848 Nouméa, New Caledonia. <sup>6</sup>CR2P/UMR 7207 (Sorbonne Université-CNRS-MNHN), 4 Place Jussieu, 75005 Paris, France. <sup>7</sup>Department of Physics and Earth Sciences, University of the Ryukyus, Okinawa, Japan. <sup>8</sup>Tokyo University of Marine Science and Technology (TUMSAT), Konan 4-5-7, Minato, Tokyo 108-8477, Japan. ✉email: laurie.charrieau@awi.de

		T (°C)	Average salinity (‰)	Average pH (pH unit)	Total alkalinity at 25 °C (μeq.kg <sup>-1</sup> )	Ω <sub>cal</sub>	[CO <sub>3</sub> <sup>2-</sup> ] (μmol.kg.sw <sup>-1</sup> )	[Ca <sup>2+</sup> ] (mmol.kg.sw <sup>-1</sup> )
Exp. 1	Tank 1	25	36.00 ± 0.00	7.94 ± 0.01	2537.86 ± 53.74	4.73	198.31	10.58
	Tank 2	25	34.33 ± 0.47	7.44 ± 0.00	2383.84 ± 10.54	1.58	65.27	10.09
	Tank 3	25	35.00 ± 0.00	6.93 ± 0.01	2458.35 ± 23.76	0.53	22.14	10.29
Exp. 2	Tank 1	25	37.33 ± 1.70	7.91 ± 0.01	2582.81	4.61	195.27	10.97
	Tank 2	25	34.00 ± 0.00	7.46 ± 0.03	2407.44 ± 7.96	1.66	68.33	9.99

**Table 1.** Water chemical variables in each tank for the two experiments. Temperature, salinity, pH and total alkalinity were measured at the beginning, middle and end of the experiment; Ω<sub>cal</sub>, [CO<sub>3</sub><sup>2-</sup>] and [Ca<sup>2+</sup>] were calculated.

the trace elements ratios to calcium in their tests usually reflects the physical and chemical conditions in the calcification environment, providing useful tools for tracking of past and present environmental changes<sup>24</sup>. Most LBF species are made of high-Mg calcite, a mineral more prone to dissolution than low-Mg calcite under low pH values<sup>25,26</sup>, and thus their elemental composition has become of increasing interest in the OA context. However, only few recent studies reported on LBF multi-elemental signatures, and contrasted effects of OA on elemental ratios (E/Ca) were observed depending on the species and on the studied carbonate system parameter<sup>27–29</sup>.

The calcification response to OA conditions is not uniform among LBF species, and notably depends on: (1) the type of symbionts they host, (2) their nutritional dependency to them, and (3) their calcification pathways (hyaline or porcelaneous forms)<sup>30</sup>. In culture experiments, the calcification rates of some hyaline species hosting diatoms were mostly unaffected and even increased under low pH conditions<sup>31–34</sup>, whereas porcelaneous species hosting dinoflagellates or chlorophytes tend to have reduced calcification rates under low pH<sup>31,32,35,36</sup>, but opposite responses were also observed<sup>33,37</sup>. Furthermore, negative synergistic and/or additive effects on the calcification process of LBF maintained in culture experiments were reported when OA conditions were combined with eutrophication<sup>38</sup>, warming<sup>39–42</sup>, or local stressor such as copper exposure<sup>43</sup>. These negative trends were confirmed by field studies implemented near naturally low pH environments such as around CO<sub>2</sub> seeps or groundwater springs, where abundance of LBF were reduced and the assemblages shifted toward non-calcifying species<sup>42,44–47</sup>. In several studies involving diverse calcifying species including SBF (Small Benthic Foraminifera), access to a sufficient food source was suggested as a crucial condition in order to cope with OA conditions<sup>6,48,49</sup>.

While many studies have focused on low pH effects on LBF survival and calcification<sup>50</sup>, fewer have investigated their potential recovery when they are subsequently put back in culture under in situ average seawater pH values. Re-calcification features after decalcification events were observed in few cases on low-Mg calcite SBF from temperate environments in both culture experiments (*Ammonia beccari*<sup>51</sup>; *Rosalina leei*<sup>52</sup>), and on the field (*Ammonia aomoriensis*<sup>53</sup>).

This study focuses on *Peneroplis* spp., a porcelaneous high-Mg calcite LBF species found free-living in tropical shallow-water environments. They host rhodophytes symbionts, giving them a light purple color<sup>15,54</sup>. Their tests have non-lamellar walls, and an outer mineralized surface (extrados) made of aligned rod-shaped crystals<sup>55</sup>. Specimens of *Peneroplis* spp. were exposed to various low pH conditions during short (3 days) and longer (1 month) culture experiments, and in dark conditions (periods called the decalcification phases). We observed the recovery of the specimens once put back under average seawater pH conditions and day/night cycles for several weeks (periods called the recovery phases), through survival and calcification's resumption abilities. In addition, two feeding treatments were tested. Decalcification and calcification's recovery features of the specimens were documented in terms of external aspect, ultrastructure, and test density, while trace element concentrations of the specimens displaying newly precipitated calcite were analyzed.

## Results

**Decalcification phases.** At the end of the decalcification phases, all the specimens displayed cytoplasm streaming and/or pseudopodia emission, and were thus considered alive. Even so, none of the specimens added new chambers during the decalcification phases. In experiment 1, after 3 days under pH 7.9 (reference conditions) or 7.4 (Ω<sub>cal</sub> > 1; Table 1), test dissolution features on the light and SEM micrographs were unclear (Fig. 1: 1, 2). However, decalcification zones were distinctly visible on the high magnification E-SEM micrographs of one of the specimens kept under pH 7.4 (Fig. 2: 2a). On these zones, the extrados layer was peeled and the randomly oriented needles-shaped crystals of the under porcelain appeared (Fig. 2: 2b). After 3 days under pH 6.9 (Ω<sub>cal</sub> < 1; Table 1), all the specimens displayed strongly decalcified tests on the light and SEM micrographs, and the inner organic lining protecting the cytoplasm and rhodophyte symbionts was largely exposed (Fig. 1: 3a, 3b). On the residual test observed by E-SEM imaging, the extrados layer was absent, and only some partly dissolved crystals of the porcelain were visible on the test surface (Fig. 2: 3b). In experiment 2, after 32 days under pH 7.4 (Ω<sub>cal</sub> > 1; Table 1), the specimens presented the most decalcified features from both experiments, and the remaining calcite was only observed near the central part and chambers' sutures of the tests (Fig. 1: 4a, b, c). The living symbionts were still clearly visible through the organic lining.

In experiment 1, test densities had on average a higher value after the 7.9 pH reference treatment compared to after the 7.4 pH treatment (1.77 and 1.67 μg/μm<sup>3</sup>, respectively; Fig. 3), which suggests loss of calcite. The average test density was the highest after the 6.9 treatment (1.81 μg/μm<sup>3</sup>). The softest parts of test being completely dissolved and therefore absent (Fig. 1: 3a, b, c), the calcite left was probably the hardest and densest, leading to the

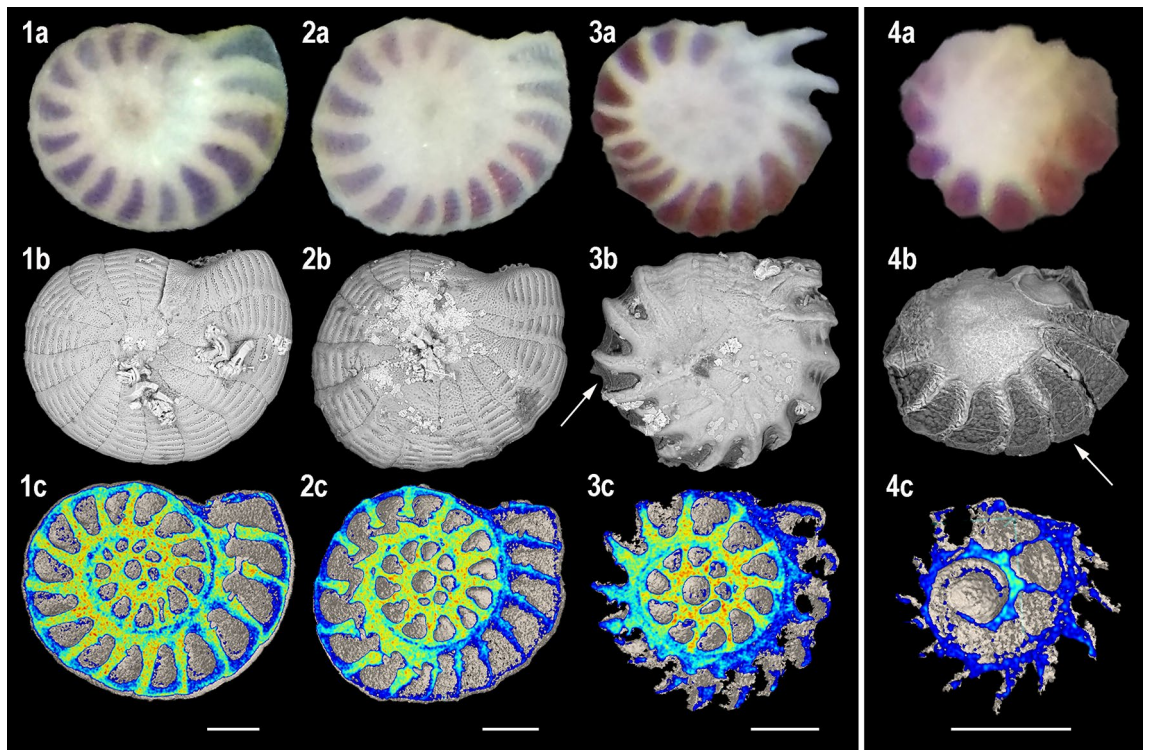


**Figure 1.** Light micrographs (above), SEM micrographs (middle) and cross-sections (below) of *Peneroplis* spp. specimens after the decalcification phases. Three days at (1) pH 7.9; (2) pH 7.4; (3) pH 6.9; (4) 32 days at pH 7.4. Colors are relative densities. Scale bars are 100  $\mu\text{m}$ . Arrows: organic lining.

overall higher densities of these specimens. At the end of experiment 2, the test density of one specimen was the lowest observed from both experiments ( $1.32 \mu\text{g}/\mu\text{m}^3$ ; Fig. 3). In that case, intense calcite loss likely happened from the whole test, including from the hardest parts (Fig. 1: 4a, b, c).

**Recovery phases.** After being back under reference pH 7.9, a new calcification phase was observed for a large majority of the specimens (Fig. 4; Table 2). This resumption of calcification took the shape of an addition of new chambers, similar to a regular calcification process. No chamber “reparations” were observed around the dissolved parts of the tests. In experiment 1, the specimens previously kept at reference pH 7.9 during the decalcification phase displayed on average 1 new chamber per specimen after the 1 month of recovery phase (Table 2). Despite being strongly decalcified, the specimens previously kept at pH 6.9 displayed on average 4 (food treatment) and 2 (no food treatment) new chambers (Fig. 4), and some specimens from the food treatment built up to 7 and 8 new chambers (Table 2). By contrast, no new chambers were observed on specimens previously kept at pH 7.4, and one specimen was considered dead at the end of the recovery phase (Table 2). In experiment 2, one specimen also died, but an average of 2 new chambers was added for the other specimens after the 15 days of recovery phase (Table 2; Fig. 4). Thus, all the specimens that resumed their calcification showed two test areas regarding calcite composition: (1) the calcite (chambers) that went through the decalcification phases and presenting varying decalcification features as described before (further called the “previous calcite”), and (2) the calcite precipitated during the recovery phases (further called the “new calcite”). Contrarily to the previous calcite, the new calcite displayed a pristine extrados layer with typical aligned rod-shaped crystals, which covers the whole surface of the newly formed chambers (Fig. 2: 4b). Despite having a pristine calcite structure, the new chambers often had abnormal size, orientation, or shape, which sometimes resulted in an altered general structure of the tests (Fig. 4: 3c, 4c, 5c). In one extreme case, a specimen showed an extra aperture after the recovery phase, which was located at the opposite side of the usual one (Fig. 2: 4a).

**Trace elements.** Due to sample availability, trace elements were only analyzed on specimens from the experiment 1. Moreover, the results report only on F and F-1 chambers of specimens that built new calcite during the recovery phase (Table 2).

Average B/Ca ratios in the new calcite of the specimens previously kept at pH 6.9 during the decalcification phase and without food treatment appeared twice smaller compared to values measured on the specimens from the reference pH 7.9 treatment, with  $145.5 \pm 39.3$  versus  $281.3 \pm 56.1 \mu\text{mol}/\text{mol}$ , respectively (Fig. 5). A similar but reversed trend was observed for Zn/Ca ratios, with the lowest average values of  $2.2 \pm 1.2$  observed on specimens from the reference treatment, while an increase to  $3.7 \pm 1.8 \text{ mmol}/\text{mol}$  could be observed on specimens from the pH 6.9 and without food treatment (Fig. 5).



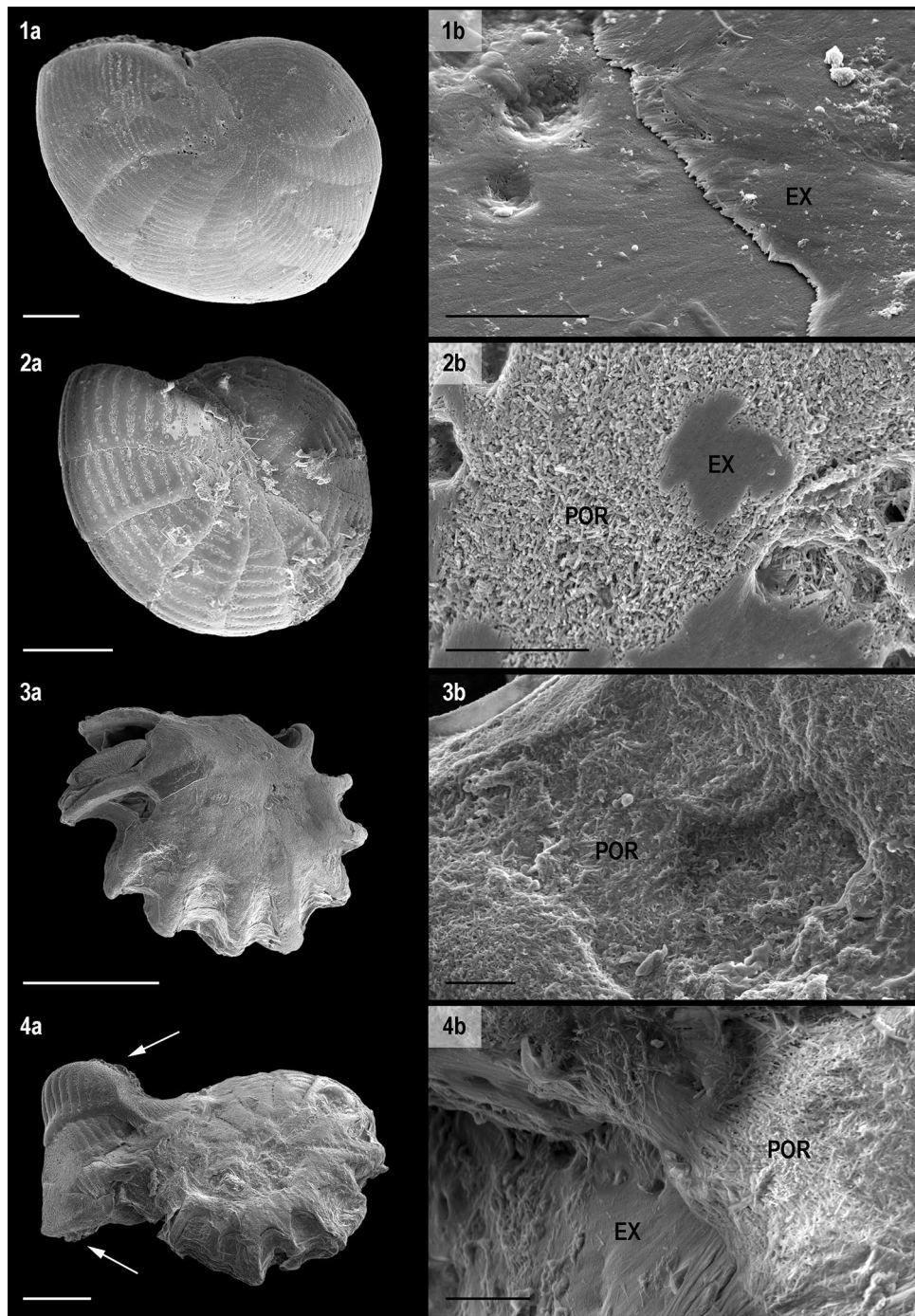


**Figure 2.** E-SEM micrographs of *Peneroplis* spp. Left: general views, scale bars are 100  $\mu\text{m}$ . Right: magnified views, scale bars are 5  $\mu\text{m}$ . Three days at (1) pH 7.9; (2) pH 7.4; (3) pH 6.9. (4) 32 days at pH 7.4 + 15 days at pH 7.9. POR porcelain, EX extrados. Arrows: apertures.

On the contrary, the average Mg/Ca ratios on the specimens from the reference pH 7.9 treatment compared to the ones from the pH 6.9 treatments were  $127.9 \pm 5.8$  and  $126.7 \pm 6.1$  mmol/mol, respectively, with no clear distinction between the two food treatments (Fig. 5). Similarly, the Sr/Ca ratios in the new calcite between the reference and lower pH treatments show no visible differences, with an average value of  $1.9 \pm 0.1$  mmol/mol for all the specimens. Including all treatments, the average Mn/Ca ratios in the newly formed chambers varied from  $94.5 \pm 59.9$  to  $173.8 \pm 142.2$   $\mu\text{mol/mol}$  (Fig. 5).

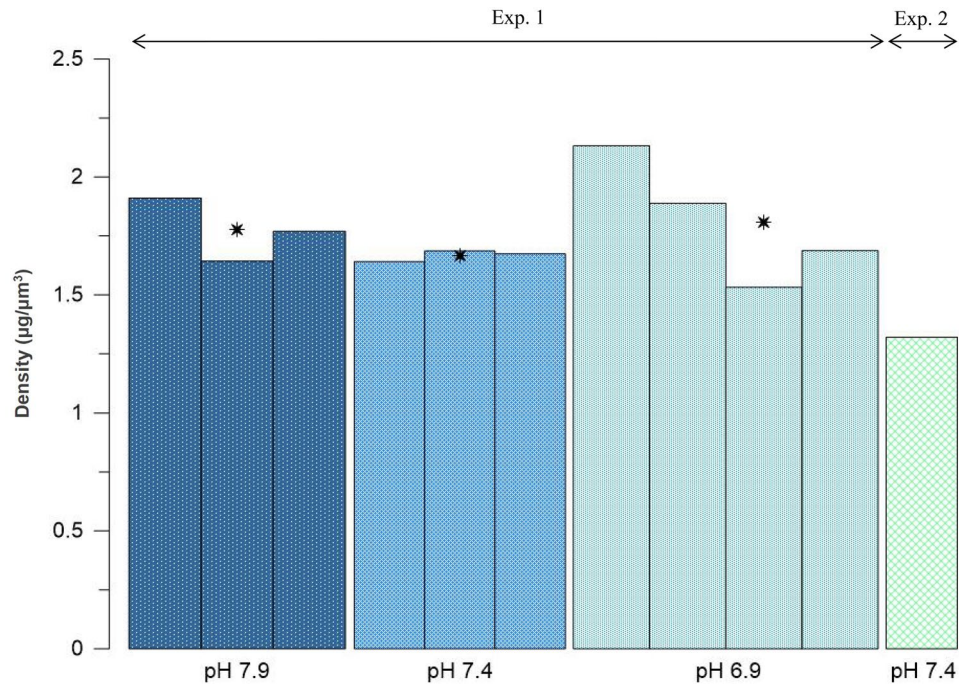


**Figure 3.** Test density of *Peneroplis* spp. specimens after 3 days at pH 7.9, 7.4 and 6.9 (Exp. 1), and after 32 days at pH 7.4 (Exp. 2). Each bar corresponds to one specimen. Stars (\*) show the mean value for each pH condition.

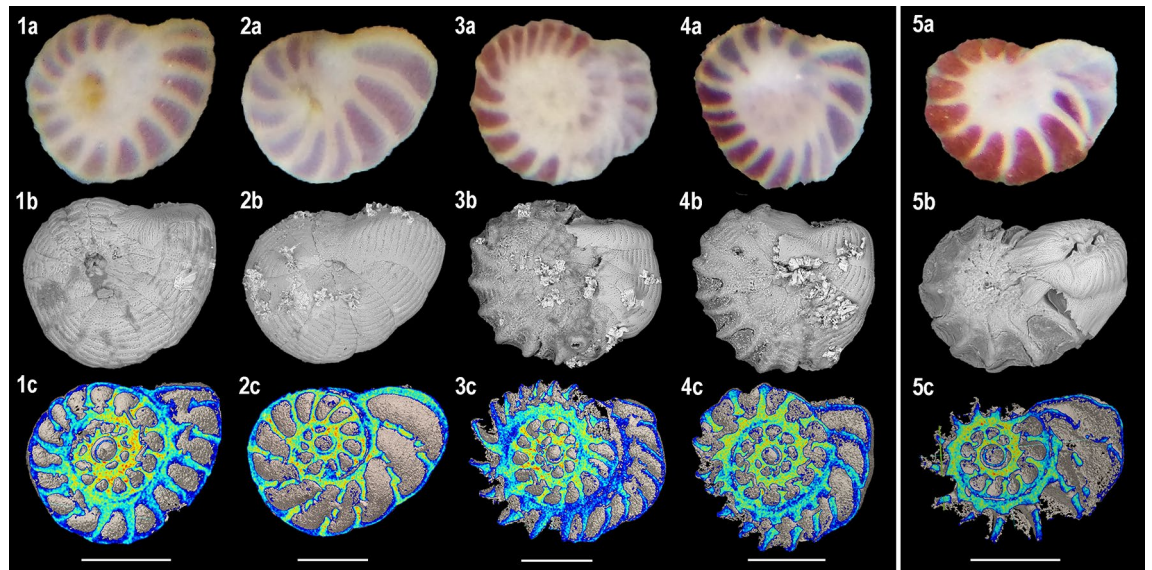


**Figure 4.** Light micrographs (above), SEM micrographs (middle) and cross-sections (below) of *Peneroplis* spp. specimens after the recovery phases. (1) 3 days at pH 7.9 + 32 days at pH 7.9, 1 new chamber; (2) 3 days at pH 7.4 + 32 days at pH 7.9, no new chamber; (3) 3 days at pH 6.9 + 32 days at pH 7.9 + food, 8 new chambers; (4) 3 days at pH 6.9 + 32 days at pH 7.9, 4 new chambers; (5) 32 days at pH 7.4 + 15 days at pH 7.9, 2 new chambers. Colors are relative densities. Scale bars are 200 µm.

## Discussion

High survival rates of LBF to short term OA conditions were previously observed in laboratory experiments, on specimens kept for several weeks under pH values between 8.2 and 7.6<sup>31,33,37</sup>. In a culture study implemented in the field, LBF specimens were able to survive at least 5 days near an hydrothermal vent where the pH was fluctuating between 7.4 and 5.9, combined with high temperature (around 40 °C<sup>42</sup>). Shores around Okinawa where our specimens were collected are dynamic environments with high pH variations, and the adaptation of *Peneroplis* spp. specimens to their in situ conditions is probably involved in their survival abilities under OA conditions<sup>7</sup>. Moreover, in all these previous experiments, day/night cycles were implemented. The symbionts



pH (time)	Experiment 1				Experiment 2
	7.9 (3 days) + 7.9 (32 days)	7.4 (3 days) + 7.9 (32 days)	6.9 (3 days) + 7.9 (32 days) + food	6.9 (3 days) + 7.9 (32 days)	7.4 (32 days) + 7.9 (15 days)
Specimen 1	1	0	8	4	3
Specimen 2	1	0	7	3	2
Specimen 3	1	0	4	2	2
Specimen 4	1	0	3	2	2
Specimen 5	0	0	2	0	0
Specimen 6	0	0 <sup>a</sup>	1	0	0
Specimen 7	-	-	-	-	0 <sup>a</sup>
Average	1	0	4	2	2

**Table 2.** Number of chambers added by *Peneroplis* spp. specimens during the recovery phase for both experiments. <sup>a</sup>Specimens that died during that phase.

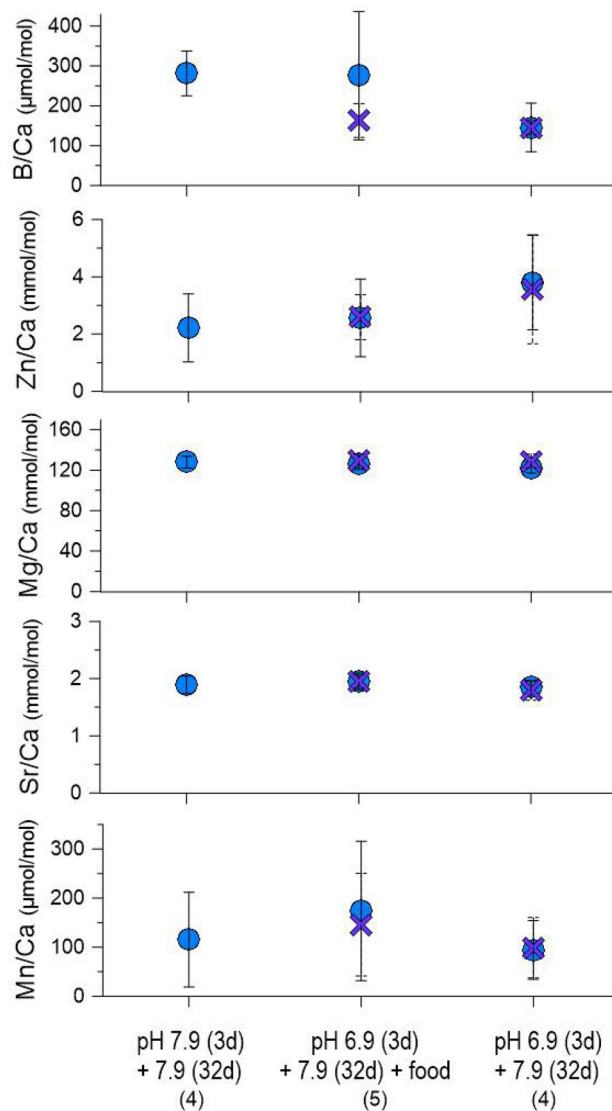


**Figure 5.** Average trace elements ratios measured on the F (blue circles) and F-1 (purple crosses) *Peneroplis* spp. chambers precipitated during the recovery phase of experiment 1. The number of specimens is indicated for each decalcification treatment. Note that the specimens from the reference pH 7.9 conditions built only one new chamber during the recovery phase, while an average of 4 and 2 chambers were built for the decalcification treatments pH 6.9 + food and pH 6.9 without food, respectively.

photosynthesis provides the specimens a significant amount of energy that is supporting their regular metabolic activities<sup>14</sup>, and they thus help the LBF to cope with stressful environments. In our experiments, all the *Peneroplis* spp. specimens were considered alive after up to 1 month under pH 7.4, and after 3 days under pH 6.9, in both cases under dark conditions and without food addition. Our observations confirm that LBF species are able to survive low pH values on the short term, even with limited energetic resources.

Even though the seawater was saturated with respect to calcite during the pH 7.4 treatment of experiment 1 (Table 1), after 3 days test densities of *Peneroplis* spp. were lower compared to after the reference conditions treatment (pH 7.9; Fig. 3), which we linked to calcite loss. Moreover, zones with peeled extrados layer were observed at high magnification (Fig. 2). Lower test densities and dissolution zones were previously reported on LBF cultured under OA conditions, and attributed to the above 1 yet decreasing  $\Omega_{\text{cal}}$  values<sup>34,36,37</sup>. On the species *Amphistegina gibbosa*, the observed dissolution zones were small and patchy<sup>34</sup>. This distribution was attributed to the ectoplasmic membrane covering the test of hyaline species that may partially protect the test from changes in the water chemistry<sup>30,56</sup>. In porcelaneous species this layer is absent, thus they might be more prone to test dissolution than hyaline species when cultured in the same conditions. In another study however, test densities were significantly lower for the hyaline species *Amphistegina lessonii* than for the porcelaneous species *Marginopora vertebralis* after exposure to low pH ( $\Omega_{\text{cal}} > 1$ <sup>37</sup>). As suggested by the authors, LBF species that have adapted to a certain pH range in situ seem unable to maintain their test integrity when exposed to acidic conditions, even in saturated conditions, as a result of an imbalance in energy investment. However, as stated in McIntyre-Wressnig et al.<sup>34</sup>, partial dissolution and lower test density appear as non-lethal effects of short term OA conditions on LBF species.

Interestingly, calcite was still present on all our specimens after 3 days under pH 6.9, despite  $\Omega_{\text{cal}}$  being below 1 (Table 1; Fig. 1: 3a, b, c). Several hyaline SBF were previously observed to survive in undersaturated conditions in culture experiments, sometimes with no signs of dissolution<sup>57–59</sup>. It has been demonstrated that some SBF have a tight control of their external and internal pH during the calcification process<sup>18–20</sup>. This ability may allow them to compensate for low pH and low  $\Omega_{\text{cal}}$  and thus maintain their tests for a certain period of time that appears to be species-specific<sup>59</sup>. On our *Peneroplis* spp. specimens, calcite was only present in small amounts after 3 days, which is supporting these previous findings.

Severe test dissolution with large parts of the test missing was observed on our specimens after 1 month under pH 7.4, in dark conditions. Similar strongly decalcified specimens exhibiting internal organic laying were reported on SBF kept under the combined effect of low pH and very low salinity<sup>52,59,60</sup>. In these experiments, most of the specimens were considered alive despite the partial to complete dissolution, as attested by feeding signs and pseudopodial activity. Living decalcified specimens were also observed on the field on SBF coastal species from temperate environments worldwide (Golfe of Mexico<sup>61</sup>; Arcachon Bay<sup>62</sup>; Baltic Sea<sup>49,53</sup>), and attributed to acidic conditions combined with other natural and/or anthropogenic stressors. In these studies however, the dissolution was linked to great decreases in general abundances<sup>49,61,62</sup>, which suggests limited survival and reproduction rates of the decalcified specimens. Therefore, if our observations suggest that a heavily decalcified test does not seem necessarily lethal at an individual level, it could still negatively impact the populations at a community level.

A new phase of calcification happened for most of our specimens when put back under in situ pH values (Table 2), which highlights the recovery abilities of *Peneroplis* spp. to OA conditions. Re-calcification events were previously observed on SBF, in culture experiments (*Ammonia beccarii*<sup>51</sup>; *Rosalina leei*<sup>52</sup>) and on the field (e.g. *Ammonia aomoriensis*<sup>53</sup>). In these studies, the calcification's resumption was described as a repair of the dissolved parts of the test. In our case, such regeneration was not observed, and instead the resuming calcification was solely an addition of new chambers. The calcification pathway of porcelaneous species such as *Peneroplis* spp. could explain this discrepancy. Indeed, unlike the hyaline species that cover their entire test with a new layer of calcite during the calcification process, porcelaneous species have non-lamellar walls which they are unable to repair following damage<sup>56</sup>. This addition of new chambers was remarkable and demonstrates the ability of *Peneroplis* spp. to absorb damages from short-term pH decrease.

Slightly dissolved specimens previously kept 3 days under pH 7.4 did not show calcification recovery features after 32 days back under in situ pH, whereas most of the individuals from the reference condition built on average 1 new chamber (Table 2). The short period of lower pH may have been a source of mild stress for the specimens, which from then might have relocated their energetic resources to respiration or homeostasis rather than calcification. By contrast, the large number of new chambers built by the heavily decalcified specimens previously kept 3 days under pH 6.9 seems to be a survival reaction after highly stressful conditions. Similar observations were made in a culture study by Le Cadre et al.<sup>51</sup>, where the partially decalcified hyaline foraminifera slowly started to re-emit pseudopodia after being placed in the rescue solution, while the strongly decalcified specimens showed an immediate and intense pseudopodia activity as soon as back at in situ pH. In the case of our 1 month under pH 7.4 treatment, such intense survival response was not observed despite the strong decalcification of the specimens, and only 2 new chambers were added on average (Table 2). This could be explained by the combination of lack of energy and time, as the recovery phase in experiment 2 lasted only 15 days and as no food was provided (see below). Thus, our data seems to indicate a threshold level regarding test dissolution/recovery of porcelaneous species, after which a survival response in the form of precipitation of new chambers is induced as soon as the specimens are placed back under more optimal pH condition.

In our experiments, the number of chambers formed during the recovery phases was on average higher when food was provided (Table 2). This is coherent with previous culture experiments where porcelaneous species showed higher growth rates in fed conditions than in unfed conditions<sup>63</sup>. A better resistance to reduced pH in terms of growth and calcification rates was observed for many other calcifiers when food was provided (review in Ref.<sup>6</sup>). Indeed, most coping mechanisms to varying pH are metabolically demanding, and this energy supply becomes then significantly important. Our results demonstrate that food supply is a crucial parameter to integrate in culture experiments in order to accurately estimate the effects of OA conditions on foraminifera.

The newly built chambers had a pristine appearance, with a perfectly calcified extrados layer (Fig. 2: 4b). Smooth surface of the re-calcified chambers compared to previous chambers was also observed in Le Cadre et al.<sup>51</sup>. However, similarly to the observations by Le Cadre et al.<sup>51</sup> and Kurtarkar et al.<sup>52</sup>, the new chambers had abnormal shape, size, or orientation, and the general structure of the tests was subsequently affected. Abnormal tests are usually attributed to stress such as pollution<sup>64</sup> or variability in the environment<sup>65</sup>, but in cases where dissolution happened, physiological or structural damages of the test during the decalcification phases were suggested<sup>52</sup>. Indeed, in foraminifera, the morphology of a new chamber is linked to the morphology of the previous chambers, so if damages have occurred on the test then the next chambers will be affected<sup>66</sup>. This was also observed many times in our laboratory during previous experiments (unpublished data). On our specimens, which already display non-repaired chambers, such deformations of the new chambers could impair their resistance to attack from other organisms as well as to physical shocks, with further serious implications for the survival and reproduction of *Peneroplis* spp. in situ.

The B/Ca ratios ( $145.4 \pm 17.6$  to  $281.3 \pm 56.1$   $\mu\text{mol/mol}$ ; Fig. 5) in our *Peneroplis* spp. were in the range of the only previously published measurement on a high-Mg calcite LBF, on the species *Amphisorus hemprichii* ( $500 \pm 204$   $\mu\text{mol/mol}$ <sup>28</sup>). In our experiment, the stress induced by 3 days under low pH 6.9 in dark conditions combined with no food given during the recovery phase has lowered the B incorporation into these specimens, in comparison to our reference conditions where specimens were maintained under pH 7.9 during the whole length of the experiment. These results are in good agreement with previous culture studies on both LBF<sup>67</sup> and planktonic foraminifera<sup>68–70</sup>, where B/Ca showed decreasing trends under lower pH. Our results highlight the LBF B/Ca signatures response to pH variations, and their potential use as a seawater carbonate chemistry proxy.

The Zn/Ca ratios measured in our *Peneroplis* spp. ( $2.2 \pm 1.2$  to  $3.8 \pm 1.7$   $\text{mmol/mol}$ ; Fig. 5) were high compared to the only ones previously observed in *P. pertusus* ( $53 \pm 10.8$   $\mu\text{mol/mol}$ <sup>27</sup>). The dark conditions during the decalcification phase in our experiment are probably involved in this offset. Indeed, Zn/Ca has been described as a nutrient proxy<sup>71</sup>, and Zn is known as an essential micronutrient for microalgae with a critical role in the photosynthesis process<sup>72</sup>. Therefore, the symbionts got probably stressed by the dark period, affecting the Zn incorporation in all our specimens. Furthermore, our results are coherent with this previous study on *P. pertusus*, where Zn/Ca ratios were also increasing under lower pH<sup>27</sup>.

The Mg/Ca ratios in *Peneroplis* spp. from our study ( $122.4 \pm 5.3$  to  $129.4 \pm 6.7$   $\text{mmol/mol}$ ) were similar to the ones in *Peneroplis planatus* (90 to 175  $\text{mmol/mol}$ <sup>73</sup>), and in *Peneroplis pertusus* ( $126.1 \pm 1.8$   $\text{mmol/mol}$ <sup>27</sup>), while our Sr/Ca ratios ( $1.8 \pm 0.2$  to  $2.0 \pm 0.1$   $\text{mmol/mol}$ ) were also comparable to previously reported values for *P. pertusus* ( $2.1 \pm 0.07$   $\text{mmol/mol}$ <sup>27</sup>). Despite the large error bars, our Mn/Ca values ( $94.5 \pm 59.9$  to  $173.8 \pm 142.2$   $\mu\text{mol/mol}$ ; Fig. 5) were in the range of concentrations observed in the high-Mg calcite LBF *Sorites marginalis* ( $61.7 \pm 27.4$   $\mu\text{mol/mol}$ <sup>74</sup>). In previous culture experiments, these three E/Ca ratios have been correlated with diverse carbonate system parameters<sup>36,57,74,75</sup>. However, in our study, the 3 days under low pH 6.9 during the decalcification phase had no visible impact on the Mg, Sr, and to a lesser extent Mn incorporation in *Peneroplis* spp. calcite during the recovery phase.

Our results suggest that the incorporation of elements such as B and Zn is rapidly impacted by a change in the environment, and only three days at lower pH and dark conditions was sufficient to modify the geochemical signature in *Peneroplis* spp. when the calcification restarts. Even though LBF E/Ca appear promising as environmental changes proxies, multi-elemental approaches and species-specific calibrations are still necessary to reinforce their reliability.

## Materials and methods

**Sampling.** Surface sediment containing live specimens of *Peneroplis* spp. was collected by hand on shores along Ikejima Island, Okinawa, Southwest Japan ( $26^{\circ} 23' \text{ N}$ ,  $128^{\circ} 00' \text{ E}$ ), in May 2019. Sediment was transported to JAMSTEC (Japanese Agency for Marine-Earth Science and Technology, Japan), and stored in its original seawater at in situ temperature (T,  $25^{\circ} \text{ C}$ ) under a 12 h day/night cycle, for one month of acclimation. During this period, salinity and pH (Total Scale) were monitored every week in the aquarium, and were on average  $36.33 \pm 1.49$  and  $7.9 \pm 0.06$ , respectively. This pH value was used as reference value in our experiments. Scarce genetic analyses were found in the literature for the *Peneroplis* genus (e.g. Ref.<sup>76</sup>), and due to the natural polymorphism observed in *Peneroplis* spp. populations, morphological identification to the species level remains unclear<sup>77,78</sup>. In this study, we use a conservative approach and refer to our specimens as *Peneroplis* spp. Reproduction happened several times in the aquarium as attested by the presence of juveniles. Adult individuals (showing at least 10 chambers) from various generations issued of reproduction within the aquarium were randomly chosen for culture experiments. The living status of selected specimens was established by direct observation of cytoplasm streaming and pseudopodia emission with a Zeiss Axio Observer Z1 inverted microscope.

**Culture experiments.** We conducted two culture experiments that are comprise both of two phases: a low pH conditions phase (called the decalcification phase), followed by a reference pH conditions phase (called the recovery phase). To avoid potential pH effects of photosynthesis by the symbionts, the decalcification phases happened in the dark. By contrast, a day/night cycle was applied during the recovery phases. A flowing system was used to ensure that the intended pH values were reaching the foraminifera microenvironment in a realistic way, as recommended for OA studies<sup>16,17</sup>. The experiments took place in an incubator that was kept constant at  $25^{\circ} \text{ C}$  during both phases.

In experiment 1, three different pH treatments were tested: 7.9, 7.4 and 6.9. We altered the pH in the three tanks by bubbling pure  $\text{CO}_2$ , in a circulating water system similar to the one described in Dissard et al.<sup>57,79</sup>, in Schiebel and Hemleben<sup>80</sup> and adapted as described in Charrieau et al.<sup>59</sup>. Culture cups (3 mL) containing 9 living specimens each were placed in the system: culture cup A in tank 1 (pH 7.9, reference conditions), culture cup



B in tank 2 (pH 7.4), and culture cups C and D in tank 3 (pH 6.9). The decalcification phase lasted 3 days. Light micrographs of each specimen were taken every day to observe survival and test dissolution features. At the end of the decalcification phase, 2 or 3 specimens from each culture cup were removed for Scanning Electron Microscope (SEM) imaging and Micro X-ray Computed Tomography (MXCT) scanning, and one specimen per condition was further selected for Environmental SEM (E-SEM) imaging. All the culture cups were then placed in reference conditions (tank 1, pH 7.9) for the recovery phase, which lasted 32 days. During this period, LBF from culture cup C were fed twice a week with *Thalassionema* sp. Light micrographs of all the specimens from the four culture cups were taken twice a week to observe survival and calcification recovery features. At the end of the experiment, SEM imaging and MXCT scanning were performed on all the specimens. Additionally, one specimen per condition was selected for E-SEM imaging, and five specimens per culture cup were selected for trace elements analysis of their tests.

In experiment 2, one culture cup E containing 12 live specimens was maintained under pH 7.4 (tank 2) for the decalcification phase, which this time lasted 32 days. At the end of the decalcification phase, one individual was removed for SEM imaging and MXCT scanning. Then, the culture cup was moved to reference conditions (tank 1, pH 7.9) for the recovery phase, which lasted 15 days. Food was not given during the second experiment. Light micrographs were taken twice a week during both phases to observe survival and decalcification/calcification recovery features. At the end of the experiment, SEM imaging and MXCT scanning were performed on all specimens and one specimen was selected for E-SEM imaging.

**Seawater carbonate chemistry.** Salinity, pH (Total Scale) and alkalinity (ALK) within the tanks were measured at the beginning, middle, and end of both experiments. ALK and pH were determined by the one point titration method described in Dickson et al.<sup>81,82</sup>, but simplified for small volumes according to in-house standards<sup>83</sup>. The water pH and HCl titrated water pH were measured with an ion meter (ORION 4 STAR, Thermo SCIENTIFIC) set with a micro composite electrode (PerpHecT<sup>®</sup> ROSS<sup>®</sup> Micro Combination pH Electrode, Thermo SCIENTIFIC). The CO<sub>2</sub>calc software program<sup>84</sup> was used to estimate other carbonate system parameters such as calcite saturation state ( $\Omega_{\text{cal}}$ ), [CO<sub>3</sub><sup>2-</sup>] and [Ca<sup>2+</sup>] (Table 1). ALK, pH, S, and T were used as inputs parameters. Equilibrium constants from Lueker et al.<sup>85</sup> were applied for K1 and K2, and total boron ratio from Uppström<sup>86</sup> was used, as recommended by Orr et al.<sup>87</sup>.

**SEM and E-SEM imaging.** The foraminifera selected for Scanning Electron Microscope (SEM) imaging were left to dry at room temperature, mounted on aluminum stubs, and placed in a Hitachi Miniscope TM3000, JAMSTEC.

Selected specimens for Environmental SEM (E-SEM) imaging were left to dry at room temperature, mounted on an aluminum stub, and covered with a thin layer of osmium coating, prior to be positioned in a Quanta 450 FEI, JAMSTEC.

Test dissolution and calcification recovery features were assessed visually by observation of the resulting images, and the specimens' images from different pH treatments were compared.

**MXCT scan.** Selected specimens for Micro X-ray Computed Tomography (MXCT) scanning were mounted on stubs and analyzed with an X-ray scanner, JAMSTEC (X-ray voltage = 80 kV, tube current = 40  $\mu$ A, target current = 10  $\mu$ A, detector matrix = 1024  $\times$  1024 pixels, 1800 projections, spatial resolution = 1.00  $\mu$ m/voxel). A grain of calcite crystal (NIST SRM8544, Limestone, NBS 19) was scanned together with each specimen as a reference standard material. We used an aluminum filter (thickness = 0.20 mm) to avoid the beam hardening effect. The Molcer-Plus software (White-Rabbit Inc, Japan) was used to reconstruct 3D and cross-section images. The CT number for each specimen was calculated and normalized based on the calcite standard values (NBS 19; 2.71  $\mu$ g/ $\mu$ m<sup>3</sup> in density; 1000 in mean CT number), using the Eq. (1):

$$\text{CT number}_{\text{sample}} = (\mu_{\text{sample}} - \mu_{\text{air}}) / (\mu_{\text{calcite}} - \mu_{\text{air}}) \times \text{CT number}_{\text{calcite}}, \quad (1)$$

where  $\mu$  is the X-ray attenuation coefficient (voxel number). The reference standard deviation (RSD) of the MXCT measurements was 0.84%.

As there is a direct relation between the CT number and the shell bulk density, we calculated the shell bulk density for each specimen using the regression Eq. (2), based on artificial calcite material with known densities:

$$\text{Bulk density } (\mu\text{g}/\mu\text{m}^3) = (\text{CT number} - 49.04) / 350.47 (R^2 = 0.999). \quad (2)$$

**Laser ablation-ICP-MS.** Foraminifera from culture experiments, alive at the time of collection, do not require the rigorous cleaning procedure applied to dead/fossil specimens. Instead, the modified cleaning procedure described in Dissard et al.<sup>57,79</sup> and Fontanier et al.<sup>88</sup> was adopted. Organic matter was removed by soaking specimens for ~35 min in a 3–7% NaOCl solution prior analysis<sup>89</sup>. Directly after complete bleaching, the specimens were thoroughly rinsed with deionized water to ensure complete removal of reagents. The last two chambers (F and F-1) of *Peneroplis* spp. specimens were analyzed (see Supplementary Fig. S1). The chambers were ablated using an Nd-YAG Laser (NWR-213, New Wave, ESI) inside an ablation chamber flushed with Helium (0.7 L/min), at the ALYSES Analytical Platform (Centre IRD France Nord). The ablated sample was then mixed with an Argon flow (0.6 L/min) and transported to an Inductively Coupled Plasma Mass Spectrometry (ICP-MS). Pulse repetition rate was set at 10 Hz, with an energy density at the sample surface of 30 J/cm. Ablation craters were 40  $\mu$ m in diameter and ablated material was analyzed with respect to time (and hence depth)

using an ICP-MS (7500cx Agilent). Two measurements were performed per chamber. Analyses were calibrated against NIST SRM 610 glass, using the concentration data of Jochum et al.<sup>90</sup> with <sup>43</sup>Ca as an internal standard. Concentrations of Mg, B, Mn, Zn, and Sr were calculated using <sup>24</sup>Mg, <sup>11</sup>B, <sup>55</sup>Mn, <sup>66</sup>Zn, and <sup>88</sup>Sr. An in-house matrix matched carbonate standard was used to verify potentially different ablation behaviour.

Received: 8 October 2021; Accepted: 1 April 2022

Published online: 16 April 2022

## References

- Caldeira, K. & Wickett, M. E. Oceanography: Anthropogenic carbon and ocean pH. *Nature* **425**, 365–365 (2003).
- Sabine, C. L. et al. The oceanic sink for anthropogenic CO<sub>2</sub>. *Science* **305**, 367–371 (2004).
- IPCC. In *IPCC Special Report on the Ocean and Cryosphere in a Changing Climate* (eds. Pörtner, H.-O., Roberts, D. C., Masson-Delmotte, V., Zhai, P., Tignor, M., Poloczanska, E., Mintenbeck, K., Alegria, A., Nicolai, M., Okem, A., Petzold, J., Rama, B., Weyer, N. M.) (2019).
- Kroeker, K. J. et al. Impacts of ocean acidification on marine organisms: Quantifying sensitivities and interaction with warming. *Glob. Change Biol.* **19**, 1884–1896 (2013).
- Ries, J. B., Cohen, A. L. & McCorkle, D. C. Marine calcifiers exhibit mixed responses to CO<sub>2</sub>-induced ocean acidification. *Geology* **37**, 1131–1134 (2014).
- Ramajo, L. et al. Food supply confers calcifiers resistance to ocean acidification. *Sci. Rep.* **6**, 19374 (2016).
- Vargas, C. A. et al. Species-specific responses to ocean acidification should account for local adaptation and adaptive plasticity. *Nat. Ecol. Evol.* **1**, 0084 (2017).
- Kleypas, J. A. & Yates, K. K. Coral reefs and ocean acidification. *Oceanography* **22**, 108–117 (2009).
- Hoegh-Guldberg, O. et al. Coral reefs under rapid climate change and ocean acidification. *Science* **318**, 1737–1742 (2007).
- Pandolfi, J. M., Connolly, S. R., Marshall, D. J. & Cohen, A. L. Projecting coral reef futures under global warming and ocean acidification. *Science* **333**, 418–422 (2011).
- Cornwall, C. E. et al. Global declines in coral reef calcium carbonate production under ocean acidification and warming. *Proc. Natl. Acad. Sci.* **118**, e2015265118 (2021).
- Langer, M. R., Silk, M. T. & Lipps, J. H. Global ocean carbonate and carbon dioxide production: The role of reef foraminifera. *J. Foraminifer. Res.* **27**, 271–277 (1997).
- Langer, M. R. Assessing the contribution of foraminiferan protists to global ocean carbonate production. *J. Eukaryot. Microbiol.* **55**, 163–169 (2008).
- Hallock, P. Symbiont-bearing Foraminifera. In *Modern Foraminifera* (ed. Sen Gupta, B. K.) 123–139 (Springer Netherlands, 2003). [https://doi.org/10.1007/0-306-48104-9\\_8](https://doi.org/10.1007/0-306-48104-9_8).
- BouDagher-Fadel, M. K. Biology and evolutionary history of larger benthic foraminifera. In *Evolution and Geological Significance of Larger Benthic Foraminifera* 1–44 (UCL Press, 2018).
- Köhler-Rink, S. & Köhl, M. Microsensor studies of photosynthesis and respiration in larger symbiotic foraminifera. I The physico-chemical microenvironment of *Marginopora vertebralis*, *Amphistegina lobifera* and *Amphisorus hemprichii*. *Mar. Biol.* **137**, 473–486 (2000).
- Glas, M. S., Fabricius, K. E., de Beer, D. & Uthicke, S. The O<sub>2</sub>, pH and Ca<sup>2+</sup> microenvironment of benthic foraminifera in a high CO<sub>2</sub> world. *PLoS One* **7**, e50010 (2012).
- De Nooijer, L. J., Toyofuku, T. & Kitazato, H. Foraminifera promote calcification by elevating their intracellular pH. *Proc. Natl. Acad. Sci. U. S. A.* **106**, 15374–15378 (2009).
- Glas, M., Langer, G. & Keul, N. Calcification acidifies the microenvironment of a benthic foraminifer (*Ammonia* sp.). *J. Exp. Mar. Biol. Ecol.* **424–425**, 53–58 (2012).
- Toyofuku, T. et al. Proton pumping accompanies calcification in foraminifera. *Nat. Commun.* **8**, 14145 (2017).
- Hallock, P., Lidz, B. H., Cockey-Burkhard, E. M. & Donnelly, K. B. Foraminifera as bioindicators in coral reef assessment and monitoring: The FORAM Index. *Environ. Monit. Assess.* **81**, 221–238 (2003).
- Uthicke, S., Thompson, A. & Schaffelke, B. Effectiveness of benthic foraminiferal and coral assemblages as water quality indicators on inshore reefs of the Great Barrier Reef, Australia. *Coral Reefs* **29**, 209–225 (2010).
- Prazeres, M., Martínez-Colón, M. & Hallock, P. Foraminifera as bioindicators of water quality: The ForAM Index revisited. *Environ. Pollut.* **257**, 113612 (2020).
- Sen Gupta, B. K. *Modern Foraminifera*. (Springer Science & Business Media, 2003).
- Morse, J. W., Andersson, A. J. & Mackenzie, F. T. Initial responses of carbonate-rich shelf sediments to rising atmospheric pCO<sub>2</sub> and “ocean acidification”: Role of high Mg-calcites. *Geochim. Cosmochim. Acta* **70**, 5814–5830 (2006).
- Andersson, A. J., Mackenzie, F. T. & Bates, N. R. Life on the margin: Implications of ocean acidification on Mg-calcite, high latitude and cold-water marine calcifiers. *Mar. Ecol. Prog. Ser.* **373**, 265–273 (2008).
- Van Dijk, I., De Nooijer, L. J. & Reichert, G.-J. Trends in element incorporation in hyaline and porcelaneous foraminifera as a function of pCO<sub>2</sub>. *Biogeosciences* **14**, 497–510 (2017).
- Not, C., Thibodeau, B. & Yokoyama, Y. Incorporation of Mg, Sr, Ba, U, and B in high-Mg calcite benthic foraminifera cultured under controlled pCO<sub>2</sub>. *Geochem. Geophys. Geosyst.* **19**, 83–98 (2018).
- Levi, A., Müller, W. & Erez, J. Intrashell variability of trace elements in benthic foraminifera grown under high CO<sub>2</sub> levels. *Front. Earth Sci.* **7**, 247 (2019).
- Doo, S. S., Fujita, K., Byrne, M. & Uthicke, S. Fate of calcifying tropical symbiont-bearing large benthic foraminifera: Living sands in a changing ocean. *Biol. Bull.* **226**, 169–186 (2014).
- Fujita, K. et al. Effects of ocean acidification on calcification of symbiont-bearing reef foraminifera. *Biogeosciences* **8**, 2089–2098 (2011).
- Hikami, M. et al. Contrasting calcification responses to ocean acidification between two reef foraminifera harboring different algal symbionts. *Geophys. Res. Lett.* **38**, L19601 (2011).
- Vogel, N. & Uthicke, S. Calcification and photobiology in symbiont-bearing benthic foraminifera and responses to a high CO<sub>2</sub> environment. *J. Exp. Mar. Biol. Ecol.* **424–425**, 15–24 (2012).
- McIntyre-Wressnig, A., Bernhard, J. M., McCorkle, D. C. & Hallock, P. Non-lethal effects of ocean acidification on the symbiont-bearing benthic foraminifer *Amphistegina gibbosa*. *Mar. Ecol. Prog. Ser.* **472**, 45–60 (2013).
- Kuroyanagi, A., Kawahata, H., Suzuki, A., Fujita, K. & Irie, T. Impacts of ocean acidification on large benthic foraminifera: Results from laboratory experiments. *Mar. Micropaleontol.* **73**, 190–195 (2009).
- Knorr, P. O., Robbins, L. L., Harries, P. J., Hallock, P. & Wynn, J. Response of the Miliolid *Archaias angulatus* to simulated ocean acidification. *J. Foraminifer. Res.* **45**, 109–127 (2015).

37. Prazeres, M., Uthicke, S. & Pandolfi, J. M. Ocean acidification induces biochemical and morphological changes in the calcification process of large benthic foraminifera. *Proc. R. Soc. B Biol. Sci.* **282**, 20142782 (2015).
38. Reymond, C., Lloyd, A., Kline, D., Dove, S. & Pandolfi, J. Decline in growth of foraminifer *Marginopora rossi* under eutrophication and ocean acidification scenarios. *Glob. Change Biol.* **19**, 291–302 (2013).
39. Sinutok, S., Hill, R., Doblin, M. A., Wuhrer, R. & Ralph, P. J. Warmer more acidic conditions cause decreased productivity and calcification in subtropical coral reef sediment-dwelling calcifiers. *Limnol. Oceanogr.* **56**, 1200–1212 (2011).
40. Sinutok, S., Hill, R., Kühl, M., Doblin, M. A. & Ralph, P. J. Ocean acidification and warming alter photosynthesis and calcification of the symbiont-bearing foraminifera *Marginopora vertebralis*. *Mar. Biol.* **161**, 2143–2154 (2014).
41. Schmidt, C., Kucera, M. & Uthicke, S. Combined effects of warming and ocean acidification on coral reef Foraminifera *Marginopora vertebralis* and *Heterostegina depressa*. *Coral Reefs* **33**, 805–818 (2014).
42. Engel, B., Hallock, P., Price, R. & Pichler, T. Shell dissolution in larger benthic foraminifers exposed to pH and temperature extremes: Results from an in situ experiment. *J. Foraminifer. Res.* **45**, 190–203 (2015).
43. Marques, J. A., de Barros Marangoni, L. F. & Bianchini, A. Combined effects of sea water acidification and copper exposure on the symbiont-bearing foraminifer *Amphistegina gibbosa*. *Coral Reefs* **36**, 489–501 (2017).
44. Uthicke, S. & Fabricius, K. E. Productivity gains do not compensate for reduced calcification under near-future ocean acidification in the photosynthetic benthic foraminifer species *Marginopora vertebralis*. *Glob. Change Biol.* **18**, 2781–2791 (2012).
45. Uthicke, S., Momiigliano, P. & Fabricius, K. E. High risk of extinction of benthic foraminifera in this century due to ocean acidification. *Sci. Rep.* **3**, 1–5 (2013).
46. Pettit, L. R., Smart, C. W., Hart, M. B., Milazzo, M. & Hall-Spencer, J. M. Seaweed fails to prevent ocean acidification impact on foraminifera along a shallow-water CO<sub>2</sub> gradient. *Ecol. Evol.* **5**, 1784–1793 (2015).
47. Martinez, A., Hernández-Terrones, L., Rebolledo-Vieyra, M. & Paytan, A. Impact of carbonate saturation on large Caribbean benthic foraminifera assemblages. *Biogeosciences* **15**, 6819–6832 (2018).
48. Pettit, L. R. *et al.* Benthic foraminifera show some resilience to ocean acidification in the northern Gulf of California, Mexico. *Mar. Pollut. Bull.* **73**, 452–462 (2013).
49. Charrieau, L. M. *et al.* The effects of multiple stressors on the distribution of coastal benthic foraminifera: A case study from the Skagerrak-Baltic Sea region. *Mar. Micropaleontol.* **139**, 42–56 (2018).
50. Narayan, G. R. *et al.* Response of large benthic foraminifera to climate and local changes: Implications for future carbonate production. *Sedimentology* <https://doi.org/10.1111/sed.12858> (2021).
51. Le Cadre, V., Debenay, J.-P. & Lesourd, M. Low pH effect on *Ammonia beccarii* test deformation: Implications for using test deformations as a pollution indicator. *J. Foraminifer. Res.* **33**, 1–9 (2003).
52. Kurtarkar, S. R., Nigam, R., Saraswat, R. & Linshy, V. N. Regeneration and abnormality in benthic foraminifer *Rosalina leei*: Implications in reconstructing past salinity changes. *Riv. Ital. Paleontol. E Stratigr.* **117**(1), 189–196 (2011).
53. Haynert, K., Schönfeld, J., Polovodova-Asteman, I. & Thomsen, J. The benthic foraminiferal community in a naturally CO<sub>2</sub>-rich coastal habitat of the southwestern Baltic Sea. *Biogeosciences* **9**, 4421–4440 (2012).
54. Lee, J. J. 'Living Sands'—Larger foraminifera and their endosymbiotic algae. *Symbiosis* **25**, 71–100 (1997).
55. Parker, J. Ultrastructure of the test wall in modern porcelaneous foraminifera: Implications for the classification of the Miliolida. *J. Foraminifer. Res.* **47**, 136–174 (2017).
56. Erez, J. The source of ions for biomineralization in foraminifera and their implications for paleoceanographic proxies. *Rev. Mineral. Geochem.* **54**, 115–149 (2003).
57. Dissard, D., Nehrke, G., Reichart, G. J. & Bijma, J. Impact of seawater pCO<sub>2</sub> on calcification and Mg/Ca and Sr/Ca ratios in benthic foraminifera calcite: results from culturing experiments with *Ammonia tepida*. *Biogeosciences* **7**, 81–93 (2010).
58. McIntyre-Wressnig, A., Bernhard, J. M., Wit, J. C. & Mccorkle, D. C. Ocean acidification not likely to affect the survival and fitness of two temperate benthic foraminiferal species: Results from culture experiments. *J. Foraminifer. Res.* **44**, 341–351 (2014).
59. Charrieau, L. M. *et al.* Decalcification and survival of benthic foraminifera under the combined impacts of varying pH and salinity. *Mar. Environ. Res.* **138**, 36–45 (2018).
60. Saraswat, R. *et al.* Effect of salinity induced pH/alkalinity changes on benthic foraminifera: A laboratory culture experiment. *Estuar. Coast. Shelf Sci.* **153**, 96–107 (2015).
61. Buzas-Stephens, P. & Buzas, M. A. Population dynamics and dissolution of foraminifera in Nueces Bay, Texas. *J. Foraminifer. Res.* **35**, 248–258 (2005).
62. Cesbron, F. *et al.* Vertical distribution and respiration rates of benthic foraminifera: Contribution to aerobic remineralization in intertidal mudflats covered by *Zostera noltei* meadows. *Estuar. Coast. Shelf Sci.* **179**, 23–38 (2016).
63. Lee, J. J. *et al.* Nutritional and related experiments on laboratory maintenance of three species of symbiont-bearing, large foraminifera. *Mar. Biol.* **109**, 417–425 (1991).
64. Yanko, V., Arnold, A. J. & Parker, W. C. Effects of marine pollution on benthic Foraminifera. In *Modern Foraminifera* 217–235 (Springer Netherlands, 1999). [https://doi.org/10.1007/0-306-48104-9\\_13](https://doi.org/10.1007/0-306-48104-9_13).
65. Polovodova Asteman, I. & Schönfeld, J. Foraminiferal test abnormalities in the western Baltic Sea. *J. Foraminifer. Res.* **38**, 318–336 (2008).
66. Boltovskoy, E. & Wright, R. The test. In *Recent Foraminifera* (eds Boltovskoy, E. & Wright, R.) 51–93 (Springer Netherlands, 1976). [https://doi.org/10.1007/978-94-017-2860-7\\_3](https://doi.org/10.1007/978-94-017-2860-7_3).
67. Kaczmarek, K. *et al.* Boron incorporation in the foraminifer *Amphistegina lessonii* under a decoupled carbonate chemistry. *Biogeosciences* **12**, 1753–1763 (2015).
68. Allen, K. *et al.* Controls on boron incorporation in cultured tests of the planktic foraminifer *Orbulina universa*. *Earth Planet. Sci. Lett.* **309**, 291–301 (2011).
69. Allen, K., Hönisch, B., Eggins, S. & Rosenthal, Y. Environmental controls on B/Ca in calcite tests of the tropical planktic foraminifer species *Globigerinoides ruber* and *Globigerinoides sacculifer*. *Earth Planet. Sci. Lett.* **351–352**, 270–280 (2012).
70. Howes, E. L. *et al.* Decoupled carbonate chemistry controls on the incorporation of boron into *Orbulina universa*. *Biogeosciences* **14**, 415–430 (2017).
71. Lea, D. W. Trace elements in foraminiferal calcite. In *Modern Foraminifera* 259–277 (Springer Netherlands, 2003).
72. Quigg, A. Micronutrients. In *The Physiology of Microalgae* (eds Borowitzka, M. A., Beardall, J. & Raven, J. A.) 211–231 (Springer International Publishing, 2016). [https://doi.org/10.1007/978-3-319-24945-2\\_10](https://doi.org/10.1007/978-3-319-24945-2_10).
73. Jennings, D. *Culturing Benthic Foraminifera to Understand the Effects of Changing Seawater Chemistry and Temperature on Foraminiferal Shell Chemistry*. (2015).
74. Van Dijk, I., De Nooijer, L. J., Barras, C. & Reichart, G.-J. Mn Incorporation in large benthic foraminifera: Differences between species and the impact of pCO<sub>2</sub>. *Front. Earth Sci.* <https://doi.org/10.3389/feart.2020.567701> (2020).
75. Raitzsch, M., Dueñas-Bohórquez, A., Reichart, G.-J., de Nooijer, L. J. & Bickert, T. Incorporation of Mg and Sr in calcite of cultured benthic foraminifera: Impact of calcium concentration and associated calcite saturation state. *Biogeosciences* **7**, 869–881 (2010).
76. Holzmann, M., Hohenecker, J., Hallock, P., Piller, W. E. & Pawlowski, J. Molecular phylogeny of large miliolid foraminifera (*Sorites* Ehrenberg 1839). *Mar. Micropaleontol.* **43**, 57–74 (2001).
77. Hottinger, L., Halicz, E. & Reiss, Z. *Recent Foraminiferida from the Gulf of Aqaba, Red Sea*. vol. 33 (Slovenska Akademija Znanosti in Umetnosti, Dela Opera, Classis IV: Historia Naturalis, 1993).



78. Langer, M., Makled, W., Pietsch, S. & Weinmann, A. Asynchronous calcification in juvenile megalospheres: An ontogenetic window into the life cycle and polymorphism of *Peneroplis*. *J. Foraminifer. Res.* **39**, 8–14 (2009).
79. Dissard, D., Nehrke, G., Reichart, G.-J. & Bijma, J. The impact of salinity on the Mg/Ca and Sr/Ca ratio in the benthic foraminifera *Ammonia tepida*: Results from culture experiments. *Geochim. Cosmochimica Acta* **74**, 928–940 (2010).
80. Schiebel, R. & Hemleben, C. *Planktic Foraminifers in the Modern Ocean*. (Springer, 2017).
81. Culberson, C. H., Pytkowicz, R. M. & Hawley, J. E. Seawater alkalinity determination by the pH method. *J. Mar. Res.* **28**, 15–21 (1970).
82. Dickson, A. G. & Goyet, C. *DOE Handbook of Methods for the Analysis of the Various Parameters of the Carbon Dioxide System in Sea Water, Version 2*. (eds., ORNL/CDIAC-74., 1994).
83. Suga, H., Sakai, S., Toyofuku, T. & Ohkouchi, N. A simplified method for determination of total alkalinity in seawater based on the small sample one-point titration method. *JAMSTEC Rep. Res. Dev.* **17**, 23–33 (2013).
84. Robbins, L. L., Hansen, M. E., Kleypas, J. A. & Meylan, S. C. *CO<sub>2</sub>calc: A User-Friendly Seawater Carbon Calculator for Windows, Mac OS X, and iOS (iPhone): U.S. Geological Survey Open-File Report 2010–1280*. 17 (2010).
85. Lueker, T. J., Dickson, A. G. & Keeling, C. D. Ocean pCO<sub>2</sub> calculated from dissolved inorganic carbon, alkalinity, and equations for K<sub>1</sub> and K<sub>2</sub>: Validation based on laboratory measurements of CO<sub>2</sub> in gas and seawater at equilibrium. *Mar. Chem.* **70**, 105–119 (2000).
86. Uppström, L. R. The boron/chlorinity ratio of deep-sea water from the Pacific Ocean. *Deep Sea Res. Oceanogr. Abstr.* **21**, 161–162 (1974).
87. Orr, J. C., Epitalon, J.-M. & Gattuso, J.-P. Comparison of ten packages that compute ocean carbonate chemistry. *Biogeosciences* **12**, 1483–1510 (2015).
88. Fontanier, C. *et al.* Living (stained) deep-sea foraminifera from the Sea of Marmara: A preliminary study. *Deep Sea Res. Part II Top. Stud. Oceanogr.* **153**, 61 (2018).
89. Gaffey, S. & Bronnimann, C. Effects of bleaching on organic and mineral phases in biogenic carbonates. *J. Sediment. Res.* **63**, 752–754 (1993).
90. Jochum, K. P. *et al.* Determination of reference values for NIST SRM 610–617 glasses following ISO guidelines. *Geostand. Geoanal. Res.* **35**, 397–429 (2011).

## Acknowledgements

We would like to thank Rika Horiuchi for technical support during Micro-CT scan analysis.

## Author contributions

L.M.C.: Design of the work, data acquisition, analysis and interpretation, manuscript draft. Y.N.: Data acquisition, manuscript edition. K.K.: Data acquisition and analysis, manuscript edition. D.D.: Data analysis and interpretation, manuscript edition. B.B.: Data acquisition, manuscript edition. K.F.: Data interpretation, manuscript edition. T.T.: Conception of the work, data interpretation, manuscript edition. All authors read and approved the final manuscript.

## Funding

Open Access funding enabled and organized by Projekt DEAL.

## Competing interests

The authors declare no competing interests.

## Additional information

**Supplementary Information** The online version contains supplementary material available at <https://doi.org/10.1038/s41598-022-10375-w>.

**Correspondence** and requests for materials should be addressed to L.M.C.

**Reprints and permissions information** is available at [www.nature.com/reprints](http://www.nature.com/reprints).

**Publisher's note** Springer Nature remains neutral with regard to jurisdictional claims in published maps and institutional affiliations.



**Open Access** This article is licensed under a Creative Commons Attribution 4.0 International License, which permits use, sharing, adaptation, distribution and reproduction in any medium or format, as long as you give appropriate credit to the original author(s) and the source, provide a link to the Creative Commons licence, and indicate if changes were made. The images or other third party material in this article are included in the article's Creative Commons licence, unless indicated otherwise in a credit line to the material. If material is not included in the article's Creative Commons licence and your intended use is not permitted by statutory regulation or exceeds the permitted use, you will need to obtain permission directly from the copyright holder. To view a copy of this licence, visit <http://creativecommons.org/licenses/by/4.0/>.

© The Author(s) 2022